数理物質科学研究科　博士論文の要約

専 攻 名　化学
学籍番号　201230088
学生氏名　大図 慎吾
学 位 名　博士（理学）
指導教員　小島 隆彦

博士論文題目 Mechanistic insights into substrate oxidations in water by ruthenium-pyridylamine complexes
（ルテニウム−ピリジルアミン錯体による水中における基質酸化反応に関する機構的考察）

Chapter 1. General Introduction

Chapter 2. Mechanistic insights into oxidation reactions of organic substrates by Ru^{IV}=O complexes in water.

Chapter 3. Highly efficient and selective photocatalytic oxidation reactions with use of Ru^{II}-OH_2 complexes as catalysts and Ru^{IV}=O complexes as reactive species

Chapter 4. Reactivity of a Ru^{III}-OH complex in substrate oxidations in water

Chapter 5. A tetranuclear Ru^{II} complex with a dinucleating ligand forming multi-mixed-valence states

Introduction

Oxidation reactions of organic substrates with metal-oxo (M=O) or metal-hydroxo (M-OH) complexes as active species have attracted considerable attention because of its relevance to biological oxidation reactions, such as enzymatic oxidations performed by cytochrome P450 and lipoxygenase having iron centers as active sites, as well as interest in those industrial applications. To gain mechanistic insights into oxidation reactions performed by aforementioned metalloenzymes, syntheses of M=O and M-OH complexes as functional models and exploration of the reactivity have been performed. One of the major procedures to form M=O and M-OH complexes is proton-coupled electron-transfer (PCET) oxidation of corresponding metal-aqua (M-OH_2) precursor complexes by using water as an oxygen source of the oxo and hydroxo ligand (Fig 1).[1] The procedure can provide one reactive species selectively to make reactions clean. However, catalytic oxidation reactions of organic substrates *via* PCET have not been well investigated until recently. Additionally, oxidation reactions with synthetic M=O and M-OH complexes have been mainly performed in organic solvents so far, whereas knowledge of those in aqueous solutions has yet to be accumulated sufficiently. Despite the fact that an association equilibrium between an enzyme such as cytochrome P450 and the specific substrate plays very important roles in the enzymatic reactions, the effects of a pre-equilibrium process to form an adduct between the oxidant and a substrate on the reactivity of M=O and M-OH complexes have been rarely investigated.

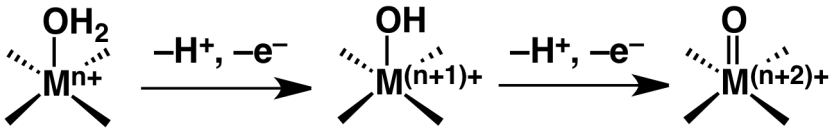

Fig 1. Synthetic procedures of metal-oxo and metal-hydroxo complexes *via* proron-coupled electron-transfer (PCET) oxidation [1].

In this thesis, oxidation reactions of organic substrates by Ru^{IV}=O and Ru^{III}-OH complexes with pyridylamine ligands in water are described to elucidate the reaction mechanism on the basis of detailed kinetic studies. In consequence, the crucial effects of an associative pre-equilibrium between the substrate and the oxidant on the oxidation reactivity have been revealed. Efficient and selective photocatalytic oxidations of various organic substrates were carried out with Ru^{II}-OH_2 complexes as oxidation catalysts, $[Ru^{II}(bpy)_3]^{2+}$ (bpy = 2,2'- bipyridine) as a photosensitizer and an electron-mediator, and a Co^{III} complex as a sacrificial oxidant. Furthermore, a novel

tetranuclear Ru^{II} complex using a dinucleating ligand was synthesized and the characteristics of the mixed-valence (MV) states were clarified.

Results and Discussion

1. Mechanistic insights into oxidation reactions of organic substrates by Ru^{IV}=O complexes in water.

Three Ru^{IV}=O complexes, **1**–**3**, employed here contain pyridylamine ligands, tris(2-pyridymethyl)amine (TPA) for **1**, [*N*,*N*-bis(2-pyridylmethyl)-*N*-(6-carboxylato-2-pyridylmethyl)amine (6-COO^--TPA) for **2**, and *N*,*N*-bis(2-pyridylmethyl)-*N*-bis(2-pyridyl)-methylamine] (N4Py) for **3** (Fig 2). Those complexes can be obtained through PCET oxidation of corresponding Ru^{II}-OH_2 precursors, $[Ru^{II}(TPA)(OH_2)_2]^{2+}$ (**4**) for **1**, $[Ru^{II}(6\text{-}COO^-\text{-}TPA)(OH_2)]^+$ (**5**) for **2**, and $[Ru^{II}(N4Py)(OH_2)]^{2+}$ (**6**) for **3**, respectively. Complexes **1**–**3** exhibit the reduction potentials of the $Ru^{III/IV}$ couples at +0.75, +0.68, +0.87 V vs SCE, respectively, at pH 1.8 in Britton-Robinson (B.-R.) buffer.

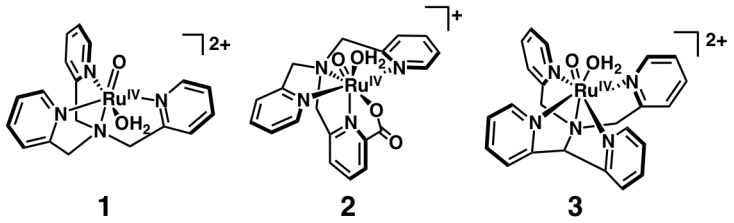

Fig 2. Strucutures of Ru^{IV}=O complexes.

Substrate oxidation reactions with **1**–**3** as oxidants were performed in the presence of an excess amount of the substrates (10–150 mM) relative to the Ru^{IV}=O species and were monitored by tracing the rise of MLCT absorptions derived from the resultant Ru^{II} species as products. In the oxidation reactions, saturation behaviors of the pseudo-first-order rate constants with respect to the concentration of substrates were commonly observed for **1**–**3** at all the temperatures examined, indicating the existence of pre-equilibrium processes prior to the oxidations. In addition, the use of hexafluoro-2-propanol (hfp) as an inert substrate with **1** allowed us to observe formation of a hydrogen-bonding adduct as demonstrated by ^{19}F NMR measurements in water. The signal of the CF_3 groups of hfp exhibited downfield shifts upon increasing the concentration of **1**, indicating that the alcohol oxygen of hfp forms hydrogen bonding with the O-H proton of **1**. This result lends credence to the adduct formation between the Ru^{IV}=O complexes and alcohols even in water.

The values of the activation parameters for the substrates oxidations were determined through variable-temperature kinetic measurements. The negatively large $\Delta S^{\ddagger}$ values suggest that the α-C–H bond of a hydrogen-bonded alcohol in the pre-equilibrium adduct may be enforced to direct to the oxo-ligand to undergo PCET reactions as hydrogen-atom transfer (HAT) *via* the formation of a tightly organized transition state. Despite the difference in bond dissociation energy (BDE) values among MeOH, 1-PrOH and 2-PrOH, the activation parameters are almost the same for the oxidations of all of the three substrates. This indicates that the rate constants for the oxidation reactions with **1**–**3** are slightly dependent on the BDEs of the C-H bonds of the substrates. To confirm the independence of the reaction rates (k) on BDE of the substrates, the rate constants for five substrates, MeOH (BDE = 96.0 kcal mol^{-1}), 1-PrOH (93.7), 2-PrOH (91.0), 4-methylbenzyl alcohol (BnOH, 87.5), sodium 4-ethylbenzene sulfonate (EtPh, 84.6), were determined at 298 K with **1** as the oxidant. A plot of log k against BDEs of the substrates showed a linear correlation (Fig 3). In most cases, rate constants of oxidation reactions with high-valent metal-oxo complexes have been demonstrated to obey the Bell-Evans-Polanyi (BEP) relation[2] to give the coefficient $\alpha \sim 0.5$: An oxidation reaction of a substrate having a larger BDE value proceeded slowly. In sharp contrast, the rate

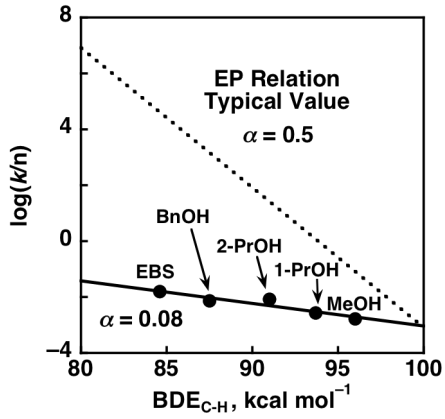

Fig 3. A plot of the log(k/n) (n: number of equivalent C-H hydrogen atoms) at 298 K for the oxidation of five substrates with **1** against BDEs of C-H bonds to be cleaved in the substrates.

constants for the oxidation reactions with **1** were almost independent on the BDE values of the substrates and the slope of the plot in Fig 3, that is α, was very small to be 0.08.

2. Highly efficient and selective photocatalytic oxidation reactions with use of Ru^{II}-OH_2 complexes as catalysts

The three Ru^{II}-aqua complexes (**4** – **6**) were revealed to be converted to corresponding Ru^{IV}=O complexes (**1** – **3**) in the presence of $[Ru^{II}(bpy)_3]^{2+}$ and $[Co^{III}Cl(NH_3)_5]^{2+}$ under photoirradiation (λ > 380 nm) in B.-R. buffer solution (pH 1.8). Photocatalytic oxidation of organic substrates was conducted at 298 K under photoirradiation (λ > 380 nm) in B.-R. buffer of D_2O (10 mM), to maintain the solution pD as 1.8, in the presence of a Ru^{II}-OH_2 complex as a catalyst (50 μM), $[Ru^{II}(bpy)_3]Cl_2$ as a photosensitizer (0.1 mM), and $[Co^{III}Cl(NH_3)_5]Cl_2$ as a sacrificial oxidant (25 mM) (Fig 4). Characterization of the products and determination of the yields were conducted by ^{1}H NMR spectroscopy after photoirradiation for 1 h. The reaction proceeded quantitatively for almost all of the substrates employed to afford a single product from one substrate and the reaction efficiencies were close to unity. In addition, the overall quantum yields (Φ) of oxidation of 4-methylbenzyl alcohol were also determined. As for the reaction in a solution of 4-methylbenzyl alcohol (10 mM) in B.–R. buffered D_2O at pD 1.8 with the catalysts (0.5 μM), $[Ru^{II}(bpy)_3]Cl_2$ (0.1 mM) and $[Co^{III}Cl(NH_3)_5]Cl_2$ (25 mM), the quantum yields determined by monitoring the formation of the product (4-methylbenzaldehyde) with use of ^{1}H NMR spectroscopy were 0.35 for **4**, 0.33 for **5**, and 0.31 for **6**, respectively.

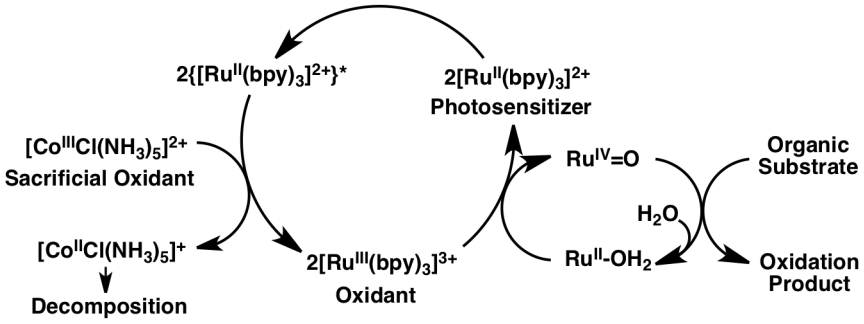

Fig 4. Photocatalytic oxidation with Ru^{IV}=O complexes.

In order to gain higher turnover numbers (TONs), photocatalytic reactions of 4-methylbenzyl alcohol as a substrate were conducted with a reduced amount of the catalysts (0.5 μM). Under the diluted conditions, TONs for complexes **4**–**6** reached over 8000; 8700 for **4**, 8240 for **5**, and 8060 for **6**. These TON values obtained here are 50–400 times higher than those of other photocatalytic systems reported so far. In order to estimate the TOF numbers of the catalytic systems, the reactions were performed at AM 1.5 using a solar simulator to fix the photoirradiation conditions. The time profiles of the product formation allowed us to determine TOFs [h^{-1}] for the three Ru^{II}-OH_2 complexes to be 13800 for **4**, 11500 for **5**, and 10500 for **6**.

3. Oxidation Reactivity of a Ru(III)-OH complex in water

A Ru^{II}-OH_2 complex with a pentadentate polypyridyl ligand, 2,6-bis{1,1-bis(2-pyridyl)ethyl}-pyridine ($PY5Me_2$), $[Ru^{II}(PY5Me_2)(OH_2)]^{2+}$, was synthesized by treatment of $[Ru^{II}Cl(PY5Me_2)]^+$ with $AgPF_6$ in water. A cyclic voltammogram (CV) of $[Ru^{II}(PY5Me_2)(OH_2)]^{2+}$ in B.-R. buffer (pH 1.8) shows a reversible oxidation wave at +0.74 V vs SCE, assigned to the Ru^{II}/Ru^{III} couple. Based on the oxidation potential, $[Ru^{III}(OH)(PY5Me_2)]^+$ (**7**) was generated from $[Ru^{II}(PY5Me_2)(OH_2)]^{2+}$ by electrochemical oxidation in B.-R. buffer (Fig 5).

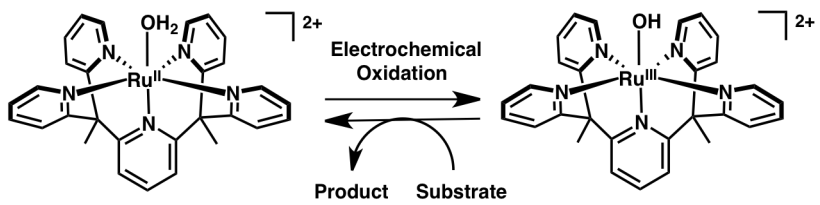

Fig 5. Formation of **7** and the oxidation reaction.

To elucidate the reactivity of **7** in oxidations of organic substrates, the reactions were performed in the presence of an excess amount of 2,5-dichloro-hydroquinone (H_2QCl_2) (25–150 mM) relative to **7** (0.5 mM) in B.–R. buffer (pH 1.8) and the rate constants were determined by tracing the rise of absorption at 380 nm derived from

the Ru^{II} species at various temperatures. In the oxidation of H_2QCl_2 with **7**, the pseudo-first-order rate constants were saturated against the concentration of H_2QCl_2 at all the temperatures examined, indicating the existence of a pre-equilibrium process prior to the oxidation. In addition, the oxidations of substrates showed KIE values for the hydroxy group to be 1.7 for H_2QCl_2 and 2,3,5,6-tetrafluoro-hydroquinone (H_2QF_4), and 1.2 for ascorbic acid (AS). The KIE values for oxidations with the three substrates indicate that the hydrogen atom abstraction from the hydroxy group is involved in the rate-determining step. Four more substrates, hydroquinone (H_2Q), 2-chloro- hydroquinone (H_2QCl), 2-fluoro-hydroquinone (H_2QF), and 2-methoxy-hydroquinone ($H_2Q(OMe)$), having lower redox potentials (–0.05 V vs SCE for H_2Q, +0.06 V for H_2QCl, +0.13 V for H_2QF, –0.18 V for $H_2Q(OMe)$) were utilized as substrates for the oxidation reactions with **7**. The larger rate constants were observed for the oxidation of H_2Q, H_2QF, H_2QCl and $H_2Q(OMe)$ than those for the oxidation of the other three substrates, due to the lower redox potentials of the four substrates. In addition, the oxidation reactions of H_2Q, H_2QF, H_2QCl and $H_2Q(OMe)$ exhibited no KIE, indicating that the oxidation reactions of the four substrates proceed through electron transfer (ET) from substrates to **7**.

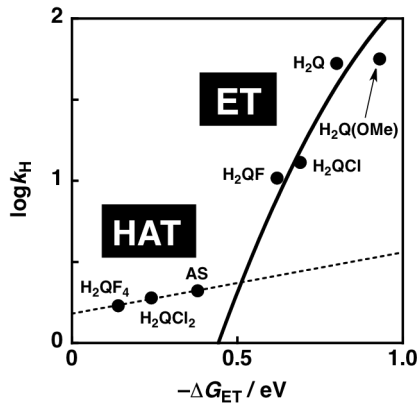

Fig 6. A plot of the logarithm of rate constants for the oxidation reactions with **7** as the oxidant against the driving forces of ET ($-\Delta G_{ET}$). All the data were determined at 297 K in B.-R. buffer (pH 1.8).

A plot of the logarithm of the rate constants at 297 K relative to the driving forces of ET ($-\Delta G_{ET}$) was made to shed light on the change of the reaction mechanism from HAT to ET in the substrate oxidation reactions by **7** (Fig 6). Substrates giving smaller $-\Delta G_{ET}$ (< 0.5 eV) are oxidized in the HAT mechanism with small driving-force dependence. In contrast, those having larger $-\Delta G_{ET}$ (> 0.5 eV) are oxidized in the ET mechanism and the rate constants fit a Marcus plot [3] for intramolecular non-adiabatic ET with λ of 1.31 eV and the electronic coupling matrix element (V) of 0.0011 cm^{-1}. The switching point of the reaction mechanisms is estimated to be located at $-\Delta G_{ET}$ = 0.51 eV.

4. A tetranuclear Ru^{II} complex with a dinucleating ligand forming multi-mixed-valence states

Synthesis of a tetranuclear Ru^{II}-bpmpm complex, $[Ru^{II}_4Cl_5(bpmpm)_2](PF_6)_3$ (**8**, bpmpm = 4,6-bis[(*N*,*N*- bis(2'-pyridylmethyl)amino)methyl]pyrimidine), was accomplished through the reaction of $[Ru^{II}Cl_2(p\text{-cymene})]_2$ with bpmpm as the dinucleating ancillary ligand in EtOH at reflux. Characterization of **8** was performed by using ESI-MS and ^1H NMR spectroscopies, and also by X-ray diffraction analysis (Fig 7). CV and DPV of **8** were measured in n-C_3H_7CN at 193 K and the CV of **8** showed four highly reversible and well-separated redox waves, assigned to Ru^{II}/Ru^{III} couples of the four Ru centers. The redox potentials ($E_{1/2}$) were determined to be +0.41, +0.78, +0.94 and +1.48 V vs SCE and electric current for each wave corresponded to that of $1e^-$-redox process based on the DPV peak intensity. The assignments were supported by the chemical oxidation experiments to observe IVCT bands.

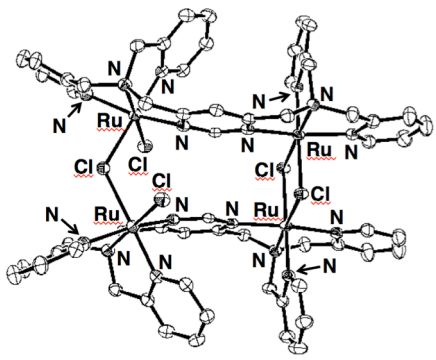

Fig 7. Crystal structure of the cationic part of **8**.

To confirm the formation of mixed-valence (MV) states for **8**, **8** was oxidized with tris(4-bromophenyl)-ammoniumyl hexachloroantimonate (TBPAH; E_{red} = +1.07 vs SCE) as a chemical oxidant. The oxidation reactions of **8** with TBPAH performed in n-C_3H_7CN at 193 K were monitored through the absorption spectral

changes. The UV-Vis spectra showed stepwise changes for addition of 0-2 equiv of the oxidant, whereas IVCT bands were not observed. In contrast, upon addition of 2-3 equiv of the oxidant, an IVCT band gradually arose at 1328 nm. Therefore, electronic coupling between Ru^{II} and Ru^{III} centers occurred in the MV state of **8** formed by $3e^-$ oxidation. The IVCT band of the $3e^-$-oxidized species of **8** disappeared upon reduction with addition of 1 equiv of decamethylferrocene (DecFc) as a chemical reductant. The comproportionation constants (K_c) of the MV states of **8** were estimated to be 1.9×10^6, 520, and 1.4×10^9 for the $1e^-$-, $2e^-$- and $3e^-$-oxidized species, respectively. In addition, the electronic coupling parameter (H_{ab}) for the $3e^-$-oxidized species of **8** was calculated to be 1868 cm^{-1}, according to the Hush equation.[4] The MV parameters indicate that the MV state formed by $3e^-$ oxidation of **8** is categorized in the Robin-Day class II, suggesting a partially valence-delocalized situation.

Summary

The reactivity of Ru^{IV}=O and Ru^{III}-OH complexes in substrate oxidations in water have been experimentally elucidated on the basis of detailed kinetic analysis. The substrate oxidation by Ru^{IV}=O (**1** – **3**) or Ru^{III}-OH (**7**) complexes involves a pre-equilibrium process involving adduct formation by hydrogen bonding between the reactive metal complex and a substrate. The driving force of the adduct formation for the Ru^{IV}=O complexes have been experimentally confirmed to be hydrogen bonding between the aqua ligand of the Ru^{IV}=O complex and an alcoholic substrate by using an inert alcohol in water for the first time. Furthermore, the significance of the adduct formation in the hydrogen abstraction reaction have been demonstrated to promote the reactions regardless of BDEs of the C-H bonds to be cleaved. All the observations for the reactions with **1** – **3** can be elucidated to involve the formation of the oxidant-substrate adduct in the pre-equilibrium process, whose structure is strictly organized by hydrogen bonding to offer large contribution of $\Delta S^{\ddagger}$ to the transition state relative to that of $\Delta H^{\ddagger}$. In addition, highly efficient and selective photocatalytic oxidation of various organic substrates has been demonstrated with use of three Ru^{II}-OH_2 complexes (**4** – **6**) as catalysts in aqueous buffered solutions. The oxidation reaction mechanism with the Ru^{III}-OH complex in water switches from HAT to ET, depending on the oxidation potentials of substrates employed. In addition, a tetranuclear Ru^{II} complex **8** having bpmpm as a dinucleating ancillary ligand exhibits stepwise oxidations to afford the three different MV states. The $3e^-$-oxidized species of **8** was assigned to be in a class II MV state.

References

[1] M. H. V. Huynh, T. J. Meyer, *Chem. Rev*. **2007**, *107*, 5004.
[2] J. M. Mayer, *Acc. Chem. Res.* **1988**, *31*, 441.
[3] R. A. Marcus, N. Sutin, *Biochim. Biophys. Acta*. **1985**, *811*, 265.
[4] N. S. Hush, *Prog. Inorg. Chem*. **1967**, *8*, 391.

List of Publications

i) S. Ohzu, T. Ishizuka, Y. Hirai, H. Jiang, M. Sakaguchi, T. Ogura, S. Fukuzumi, T. Kojima, *Chem. Sci*. **2012**, *3*, 3421.
ii) S. Ohzu, T. Ishizuka, Y. Hirai, S. Fukuzumi, T. Kojima, *Chem.−Eur. J.* **2013**, *19*, 1563.
iii) T. Ishizuka, S. Ohzu, H. Kotani, Y. Shiota, K. Yoshizawa, T. Kojima, *Chem. Sci*. **2014**, *5*, 1429.
iv) S. Ohzu, T. Ishizuka, H. Kotani, T. Kojima, *Chem. Commun*. **2014**, *50*, 15018.
v) S. Ohzu, T. Ishizuka, H. Kotani, Y. Shiota, K. Yoshizawa, T. Kojima, *Inorg. Chem.* **2014**, *53*, 12677.

Supplementary Publications

1) Y. Shiota, J. M. Herrera, G. Juhasz, T. Abe, S. Ohzu, T. Ishizuka, T. Kojima, K. Yoshizawa, *Inorg. Chem*. **2011**, *50*, 6200.
2) M. Makino, T. Ishizuka, S. Ohzu, H. Jiang, H. Kotani, T. Kojima, *Inorg. Chem*. **2013**, *52*, 5507.
3) T. Ishizuka, S. Ohzu, T. Kojima, *Synlett* **2014**, *25*, 1667.
4) Y. Shiota, S. Takahashi, S. Ohzu, T. Ishizuka, T. Kojima, K. Yoshizawa, *J. Porphyrins Phthalocyanines* **2015**, in press.